Magnetoacoustic attenuation in the mixed state of Nb–26-at.% Hf†

F. P. Missell*‡ and N. F. Oliveira, Jr.
Instituto de Física, Universidade de São Paulo, C.P. 20516, São Paulo, S.P., Brasil

Y. Shapira
Francis Bitter National Magnet Laboratory,§ Massachusetts Institute of Technology, Cambridge, Massachusetts 02139
(Received 5 April 1976)

The ultrasonic attenuation in the mixed state of Nb–26-at.% Hf was measured at $T = 4.14$ K, using shear and longitudinal waves with frequencies 5–140 MHz. The experimental data are incompatible with the microscopic theories of Houghton and Maki, and of Cerdeira and Houghton. On the other hand, the magnetic-field and frequency dependence of the attenuation agree well with a phenomenological model of Shapira and Neuringer in which magnetohydrodynamic effects are included. We have also modified the original model of Shapira and Neuringer, using Thompson's result for the flux-flow resistivity as an effective resistivity in the Alpher-Rubin theory. We thus obtained an expression for the mixed-state attenuation, valid for $H \sim H_{c2}$ and for high frequencies such that the pinning forces may be neglected. This modification improves the agreement with experimental data for the magnetic-field dependence of the attenuation.

I. INTRODUCTION

Ultrasonic attenuation has proved to be valuable in elucidating the properties of superconductors. Historically, measurements of the ultrasonic attenuation in type-I superconductors provided one of the initial confirmations of the BCS theory and were also used to measure the energy gap.[1] Later, attention was focused on the attenuation in the mixed state of type-II superconductors.[2] More recently, Houghton and Maki (HM)[3] and Cerdeira and Houghton (CH)[4] made predictions concerning the dependence of the mixed-state attenuation on magnetic field, temperature, and purity of the sample. These predictions have been substantially verified for Nb,[5] V,[6] and other materials.[7,8] These superconductors had relatively low upper critical fields H_{c2}. The attenuation in superconductors with much higher upper critical fields was studied by Shapira and Neuringer (SN) who emphasized the importance of magnetohydrodynamic effects at high fields.[9,10]

In a recent article[11] we compared the measured attenuation of transverse ultrasonic waves in the mixed state of Nb–26-at.% Hf with theoretical calculations by HM and CH. We showed that our experimental data could not be interpreted in terms of these theories. According to HM and CH, the quantity $\Delta\alpha/\alpha_n = (\alpha_n - \alpha_s)/\alpha_n$ (where α_s is the electronic contribution to the attenuation in the mixed state and α_n is the normal attenuation) is positive for $H \lesssim H_{c2}$. Furthermore, these theories predict that $\Delta\alpha/\alpha_n$ is independent of the ultrasonic frequency, provided that $ql < 1$, where q is the wave vector of the sound wave and l is the electronic mean free path. In contrast with those predictions, our experiments in Nb–26-at.% Hf showed that $\Delta\alpha/\alpha_n$ is in many cases *negative* for large portions of the mixed state and is strongly dependent upon frequency, especially for lower frequencies. In the present work, we show that the same inconsistencies exist between the theories of HM and CH and the mixed-state attenuation of longitudinal waves. That is, using longitudinal waves, we find that $\Delta\alpha/\alpha_n$ may be negative for large portions of the mixed state and is strongly dependent upon frequency.

In Ref. 11 we also compared our experimental results with a phenomenological model for the attenuation in the mixed state which was proposed by SN. These authors used a simplified form for the ac resistivity associated with flux-line motion in the mixed state[12,13] as an effective resistivity in the Alpher-Rubin (AR) theory[14] to obtain an expression for the attenuation in the mixed state. In the AR theory, which describes the influence of a magnetic field on sound propagation in a normal metal, the change in the attenuation due to an external magnetic field H is given in terms of a parameter $\beta = 2\pi^2(\delta/\lambda)^2$, where δ is the classical skin depth and λ is the ultrasonic wavelength. In the model of SN, the effective skin depth depends upon the motion of flux lines in the mixed state and is, therefore, a function of both the magnetic field H and the strength of the pinning forces. The latter strength is characterized by a characteristic frequency ω_0 which depends on the metallurgical properties of the material.

Previously we showed that the frequency dependence of shear-wave attenuation was in good agreement with the model of SN. In the present work, we make more extensive comparisons of our experimental data to the predictions of this model and show that it is in good qualitative agreement

with the magnetic field and frequency dependences of the attenuation. This work is the first quantitative study of the frequency dependence of the attenuation in the mixed state, and it strongly supports the SN model for the attenuation in the mixed state of high-field superconductors. In addition, we find that a single characteristic frequency or "depinning frequency"[9,10] ω_0 is adequate to describe the attenuation measurements with both shear and longitudinal waves. Finally, the magnitude of the characteristic frequency ω_0 is in good agreement with the value predicted by this model.

The model of SN gives a good description of the mixed-state attenuation, especially for frequencies in the vicinity of the characteristic frequency ($f_0 = \omega_0/2\pi \sim 10$–$15$ MHz in our Nb–26-at.% Hf for $T = 4.14$ K). It is well known, however, that for much higher frequencies, the effects of pinning forces can be neglected.[12] For this case of no pinning the flux-flow resistivity just below the upper critical field H_{c2} has been calculated by Thompson,[15] who corrected the earlier calculations of Caroli and Maki.[16,17] The necessity of Thompson's corrections to the Caroli-Maki theories has subsequently been verified by Takayama and Ebisawa.[18] Thompson's theory for the flux-flow resistivity in the absence of pinning forces is expected to give more accurate results than the phenomenological models[12,19] available when the SN theory for the mixed-state attenuation was formulated. We have, therefore, modified the original model of SN, using Thompson's result for the flux-flow resistivity as an effective resistivity in the AR theory. Our result for the mixed-state attenuation should be valid for magnetic fields $H \lesssim H_{c2}$, and for high frequencies such that the effects of pinning may be neglected. Our modification improves the agreement with experimental data for the magnetic-field dependence of the attenuation, eliminating the discontinuity in α_s/α_n at H_{c2} predicted by the model of SN. Furthermore, our model correctly predicts the linear dependence of α_s/α_n on H for fields just below H_{c2} when $\beta \gg 1$. (See Note added in proof.)

The success of these models in describing the mixed-state attenuation is consistent with recent experiments involving the electromagnetic generation and detection of ultrasonic waves in superconductors. For example, Vienneau and Maxfield[20] explained their observations of electromagnetic detection in terms of a local model based upon the Lorentz force acting upon currents induced within the electromagnetic skin depth. With decreasing magnetic field, the electromagnetic screening in the mixed state becomes more effective, i.e., the skin depth decreases from its normal-state value (above H_{c2}) to the London penetration depth at zero field. In the case of the ultrasonic attenuation, the situation is analogous. The effective skin depth is essentially magnetic field dependent and this H dependence has importance consequences for the ultrasonic attenuation in terms of the AR theory.

II. THEORY

A. Model of Shapira and Neuringer

In this section we wish to recall certain results, obtained previously by SN,[9,10] which will be useful in later discussions. We first note that the AR theory,[14] which is appropriate for normal metals, gives only the H-induced change in the ultrasonic attenuation, i.e., the zero-field attenuation is ignored. Later, we will estimate the electronic contribution to the zero-field attenuation for Nb–26-at.% Hf and show that it is much smaller than the H-induced change in the attenuation for $H \sim H_{c2}$. Therefore it is a good approximation to neglect the electronic attenuation in the absence of a field. We do this in what follows and denote the H-induced change in the normal attenuation by α_n.

For $H > H_{c2}$, the superconductor is in the normal state and the AR theory is expected to be valid. For shear waves with $\vec{q} \| \vec{H}$ and for longitudinal waves with $\vec{q} \perp \vec{H}$, this theory gives[9,10]

$$\alpha_n = (\omega H^2 \mu/8\pi d V^3)[\beta/(1+\beta^2)] \ \text{(Np/cm)}\,, \qquad (1)$$

where d is the density of the sample, V is the zero-field sound velocity (V_L for longitudinal waves and V_S for shear waves), ω is the angular frequency of the sound wave, and μ is the permeability. The parameter β is given by

$$\beta = c^2 \omega \rho_n/4\pi\mu V^2 = 2\pi^2(\delta/\lambda)^2\,, \qquad (2)$$

where ρ_n is the normal-state resistivity. In the normal state, μ is very nearly equal to unity and we make this approximation in what follows.

It is interesting to note that α_n depends upon the normal resistivity through the factor $\beta/(1+\beta^2)$, since β is proportional to ρ_n. Thus, for a fixed ω, the normal attenuation has a maximum with respect to ρ_n when the normal resistivity is such that $\beta = 1$. Physically this means that the normal attenuation is maximum when the classical skin depth δ is comparable with the ultrasonic wavelength λ.

The main assumption of the SN model is that the attenuation in the mixed state can be obtained from the AR theory by replacing the normal electrical resistivity by the mixed-state resistivity for a frequency ω equal to that of the sound frequency. In typical normal metals, where the electron mean free path is very small, the normal resistivity for frequencies up to ~ 100 MHz is essentially a real quantity. In contrast, in the mixed state of a type-

II superconductor, the ac resistivity is, in general, a complex quantity and it is necessary to generalize Eq. (1) in the appropriate manner. If one assumes that $\rho = \rho_1 + i\rho_2$, then for shear waves with $\vec{q} \| \vec{H}$ and longitudinal waves with $\vec{q} \perp \vec{H}$ one obtains

$$\alpha = (\omega H^2 \mu / 8\pi d V^3) \{\beta_1 / [(1+\beta_2)^2 + \beta_1^2]\} \quad (\mathrm{Np/cm}), \tag{3}$$

where

$$\beta_1 = c^2 \omega \rho_1 / 4\pi \mu V^2, \quad \beta_2 = c^2 \omega \rho_2 / 4\pi \mu V^2. \tag{4}$$

To obtain an expression for the mixed-state attenuation, SN employed in Eq. (3) an effective ac resistivity for the mixed state, derived from a phenomenological model due to Gittleman and Rosenblum.[12] For $H_{c1} \ll H < H_{c2}$, the complex resistivity is given by

$$\rho = \rho_1 + i\rho_2 = \rho_f (1 + ir)/(1 + r^2), \tag{5}$$

where ρ_f is the dc flow resistivity[19] and $r = \omega_0/\omega$. For $H_{c1} \ll H < H_{c2}$ the phenomenological theories for the flow resistivity give[19]

$$\rho_f = \rho_n H / H_{c2}^*(0). \tag{6}$$

Here $H_{c2}^*(0)$ is the upper critical field at $T = 0$ K which would have been present in the absence of Pauli paramagnetism. When the upper critical field is not limited by Pauli paramagnetism, $H_{c2}^*(0)$ in Eq. (6) can be replaced by $H_{c2}(0)$, the actual upper critical field at $T = 0$ K. The characteristic frequency ω_0 can be estimated from the critical current density J_c:

$$\omega_0 \cong 2\pi J_c \rho_n c H^{1/2} / H_{c2}^*(0) \phi_0^{1/2}, \tag{7}$$

where ϕ_0 is the flux quantum $hc/2e$.[9,10,12]

Using these results SN obtained an expression for the mixed-state attenuation:

$$\alpha_s = (\omega H^2 \mu / 8\pi d V^3) \times \{\beta_f (1+r^2) / [(1 + r^2 + r\beta_f)^2 + \beta_f^2]\} \quad (\mathrm{Np/cm}), \tag{8}$$

where

$$\beta_f = c^2 \omega \rho_f / 4\pi \mu V^2. \tag{9}$$

Equation (8) should be valid for $H_{c1} \ll H < H_{c2}$. In this region the magnetic induction B is nearly equal to H, so that to a good approximation $\mu = 1$. In comparing our experimental results to this model, it is convenient to consider the quantity α_s/α_n, obtained by dividing Eq. (8) by Eq. (1):

$$\alpha_s/\alpha_n = \beta_f (1+r^2)(1+\beta^2) / \beta [(1 + r^2 + r\beta_f)^2 + \beta_f^2]. \tag{10}$$

Note that all quantities appearing in Eq. (10) can be determined experimentally and, therefore, this model involves no adjustable parameters.

B. Extension of the model

The work of Kim *et al.*[19] suggests that Eq. (6) for the flux-flow resistivity should be valid only for low reduced temperatures $t = T/T_c$ and for magnetic fields not too close to H_{c2}. In fact, a number of authors have studied the deviations from Eq. (6) in the vicinity of H_{c2}.[21,22] In the case of ultrasonic attenuation, the apparent discontinuity in ρ at H_{c2}, suggested by Eq. (6), would lead to a discontinuity in the attenuation at H_{c2}. As we will demonstrate later, this behavior is not observed.

A calculation of the flux-flow resistivity $\rho_f(\omega)$ for magnetic fields in the vicinity of H_{c2} has been carried out by Thompson,[15] starting from the time-dependent Ginzburg-Landau equation. Neglecting effects due to the pinning of flux lines, Thompson related the current $\vec{J}$ in the superconductor to the vector potential $\vec{A}(t) = \vec{A}_\omega e^{-i\omega t}$ by means of a response function Q, such that $\vec{J} = -Q\vec{A}$. In this case, the conductivity of the medium is given by $\sigma(\omega) = -Q/i\omega$. He then calculated the most important correction Q' to the response function of the normal state Q_n for magnetic fields in the vicinity of H_{c2}. To improve on the SN model, we use Thompson's result for $\sigma(\omega)$ as an effective conductivity in the AR theory and thus obtain an expression for the mixed-state attenuation. This expression is valid only for frequencies such that pinning effects may be neglected (i.e., $\omega \gg \omega_0$) and for $H \lesssim H_{c2}$. In this work we are concerned only with shear waves with $\vec{q} \| \vec{H}$ and longitudinal waves with $\vec{q} \perp \vec{H}$. It therefore seems appropriate to consider the result for Q' obtained by Thompson for the external field $\vec{H}$ normal to the sample surface and perpendicular to the rf electric field. In the dc limit, this result gives the dc flux-flow resistivity. For the temperatures and frequencies of our experiments, the condition $\hbar\omega \ll k(T_c - T)$ for the dc limit is easily satisfied. In this case, the appropriate expressions for Q' are given by Eqs. (7a) and (7b) of Pedersen *et al.*[23]

$$(\mathrm{Re}Q')/\omega = 0 \tag{11a}$$

and

$$(\mathrm{Im}Q')/\omega = ecML_D(t)/2\pi kT\eta. \tag{11b}$$

In these equations, M is the magnetization, which, for $H \lesssim H_{c2}$, is given by[24]

$$-4\pi M = (H_{c2} - H)/[1.16(2\kappa_2^2 - 1) + N], \tag{12}$$

where N is the demagnetization factor and κ_2 is the second Ginzburg-Landau parameter. Also in Eq. (11b) we have

$$\eta = eDH_{c2}(t)/2\pi ckT, \tag{13}$$

where $D = \frac{1}{3} v_F l$ is the diffusion constant. The dif-

ference between Thompson's result and that of the second calculation of Caroli and Maki[17] lies in the factor $L_D(t)$ which is given by

$$L_D(t) = 2 + \eta\psi''(\tfrac{1}{2}+\eta)/\psi'(\tfrac{1}{2}+\eta)\,, \tag{14}$$

where ψ' and ψ'' are the first and second derivatives of the digamma function ψ. This factor $L_D(t)$ varies continuously between $T=0$ K, where $L_D(t)=1$, and $T=T_c$, where $L_D(t)=2$.

Combining these results, one obtains the resistivity for $H \lesssim H_{c2}$:

$$\rho = \rho_n/[1+\gamma(1-H/H_{c2})] = \rho_n/g\,, \tag{15}$$

where

$$\gamma = c^2\rho_n L_D(t)/4\pi D[1.16(2\kappa_2^2-1)+N]\,. \tag{16}$$

In Sec. IV C it is shown that γ is of the order of unity for our Nb–26-at.% Hf. We defined also the quantity g by

$$g = 1+\gamma(1-H/H_{c2})\,. \tag{17}$$

At this point we use ρ, given by Eq. (15), as an effective resistivity in Eq. (3) and, with Eq. (1), obtain

$$\alpha_s/\alpha_n = g(1+\beta^2)/(g^2+\beta^2)\,. \tag{18}$$

In the limit of high frequencies where $\omega \gg \omega_0$ and $\beta \gg 1$, Eq. (18) simplifies to

$$\alpha_s/\alpha_n \simeq g = 1+\gamma[1-(H/H_{c2})] \tag{19}$$

for H just below H_{c2}. This result says that the quantity α_s/α_n depends linearly upon the difference $(H_{c2}-H)$ for magnetic fields in the vicinity of H_{c2}.

As we mentioned earlier, the difference between Thompson's result and that of the second calculation of Caroli and Maki[17] lies in the factor $L_D(t)$. However, we must recall the ranges of validity of these two theories. As Thompson pointed out,[15] the Caroli-Maki result, which includes products of only advanced or of only retarded Green's functions, is valid for magnetic fields such that $1-H/H_{c2}(t) \ll 1$. Thompson's result, which also includes products of advanced and retarded Green's functions, has a somewhat narrower range of validity: $1-H/H_{c2}(t) \ll H_{c2}(t)/H_{c2}(0)$. Thus, in comparing Eq. (18) with our experimental results, we must consider magnetic fields very close to $H_{c2}(t)$.

III. EXPERIMENTAL TECHNIQUE AND PHYSICAL PROPERTIES OF Nb–26-at.% Hf

The polycrystalline sample used in the present work was cut from a speciman of Nb–26-at.% Hf, kindly provided by L. J. Neuringer. The original speciman had been prepared by combining the constituents in an electric arc furnace, after which the alloy was vacuum-annealed at 1800 °C for 16 h.

Ultrasonic attenuation measurements were made using conventional pulse-echo techniques. We estimate that the H-induced attenuation changes were measured with an accuracy of 10%. Transit times, to determine the sound velocity, were obtained using the pulse-echo overlap method.[25] For $T=4.14$ K, the velocity of shear waves is $V_S = (2.006\pm0.007)\times10^5$ cm/sec and for longitudinal waves $V_L = (4.56\pm0.02)\times10^5$ cm/sec. The experimental uncertainties associated with the velocities reflect, principally, the uncertainity in the thermal contraction which is needed for an accurate determination of the sample's length. (We should mention that these values for V_S and V_L differ slightly from previously quoted results[26] because of errors in the previous measurements. However, the conclusions of Ref. 26 are not affected by these differences.) The density d of the sample was measured at room temperature. Assuming a volume correction for thermal contraction of ~1%, we found $d = 10.1\pm0.1$ g/cm^3 for $T=4.14$ K. Using the velocities V_S and V_L and the density of the sample, we have determined for Nb–26-at.% Hf, Young's modulus $Y = (1.12\pm0.01)\times10^{12}$ dyn/cm^2, the Poisson ratio $\nu = 0.380\pm0.001$, and the adiabatic compressibility $K_S = (6.43\pm0.08)\times10^{-13}$ cm^2/dyn. From Anderson's equation for the Debye temperature Θ_D of an isotropic material,[27] we calculate $\Theta_D = 254\pm2$ K.

The phase diagram (H_{c2} vs T) of Nb–26-at.% Hf was determined from resistivity measurements carried out using standard four-wire techniques. The criterion for H_{c2} was chosen to be the zero-voltage intercept of the linear portion of the transition on a voltage-versus-field curve. Since the width of the resistive transition was small (~1.5 kOe) and did not vary appreciably with temperature, it seems reasonable that the use of another criterion would have led to essentially the same results. In Fig. 1 we present the phase diagram determined from our resistive measurements. An extrapolation of the experimental points to $H_{c2}=0$ gives the critical temperature $T_c = 9.3\pm0.1$ K which agrees with Hulm and Blaugher.[28]

Using the relation of Maki,[29]

$$H_{c2}^*(0) = -0.69T_c\left(\frac{dH_{c2}}{dT}\right)_{T=T_c}\,, \tag{20}$$

we obtained the upper critical field in the absence of paramagnetic limiting: $H_{c2}^*(0) = 68.6\pm2$ kOe. For low values of the reduced temperature $t=T/T_c$, the dependence of the observed critical field on t is parabolic. The empirical relation, determined from a fit to the experimental points for $t \lesssim 0.26$, is $H_{c2}(t) = H_{c2}(0)(1-1.89t^2)$ with $H_{c2}(0) = 74.5$ kOe. We note that the extrapolated value $H_{c2}(0)$ is some-

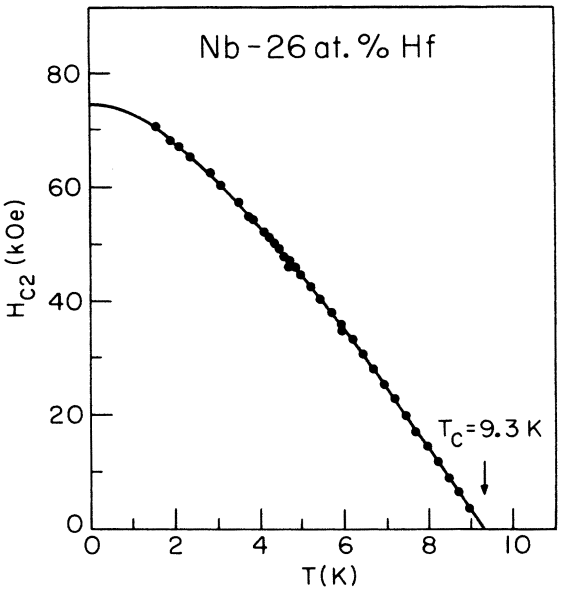

FIG. 1. Temperature dependence of H_{c2} for Nb–26-at.% Hf as determined from resistive measurements. The solid line was drawn through the experimental points. T_c was obtained by extrapolating this line to $H_{c2}=0$.

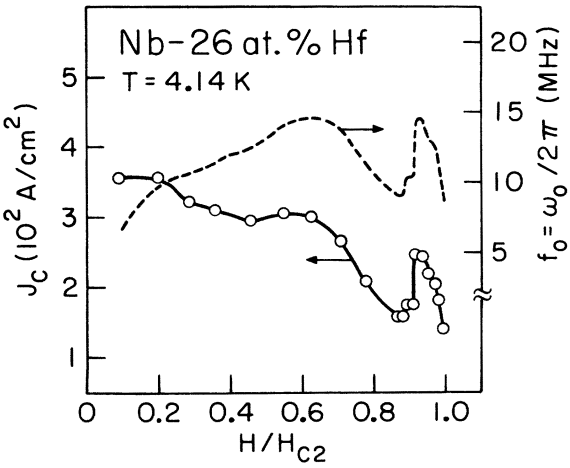

FIG. 2. Critical current J_c (open circles) vs H at $T=4.14$ K. The peak in J_c at $H/H_{c2}\simeq 0.9$ is the "peak effect." The characteristic frequency $f_0(H)=\omega_0(H)/2\pi$ (dashed curve) was calculated from J_c using Eq. (7).

what larger than the value $H_{c2}^{*}(0)$, obtained from Maki's relation.[29] This cannot be explained in terms of the theories of Maki and of Werthamer *et al.*[30] However, the recent work of Somekh[31] has shown that effects related to the anisotropy of the Fermi surface may be important in "dirty" superconductors.

Attempts were made to measure the magnetization of the sample using a vibrating-sample magnetometer. However, the experimental curves were highly irreversible and it was not possible to determine the area under the magnetization curve. On the other hand, a sharp maximum was observed in the curve of $-4\pi M$ versus applied field, and this maximum was identified with H_{c1}. For $T=4.14$ K, we found $H_{c1}=0.9$ kOe. Using this value for H_{c1}, and the measured value of H_{c2} for $T=4.14$ K, we estimated[32] $\kappa_2=7.4$ for Nb–26-at.% Hf for $T=4.14$ K.

To characterize superconductivity in the alloy Nb–26-at.% Hf, we estimated the value of $2\Delta/kT_c$, where 2Δ is the energy gap at $T=0$ K. Using the empirical relation of Laibowitz *et al.*,[33] we related T_c/Θ_D to $2\Delta/kT_c$, obtaining $2\Delta/kT_c=3.7$. This is slightly larger than the BCS prediction for the same quantity. Our experimental value for T_c/Θ_D also allowed us to estimate the value of Λ, the parameter which characterizes the electron-phonon coupling. An explicit expression for Λ is given in Eq. (30) of McMillan[34] in terms of T_c/Θ_D and ζ, the Coulomb pseudopotential. Using the value $\zeta=0.13$, which is appropriate for transition metals,[34] we obtained $\Lambda=0.86$, which corresponds to an intermediate electron-phonon coupling.

In order to make a quantitiative comparison between our measurements of the mixed state attenuation and the model of SN, it is necessary to measure the critical current density J_c so that the characteristic frequency ω_0 may be estimated using Eq. (7). The critical current density was determined for $T=4.14$ K, as a function of the applied magnetic field, in the usual geometry with the current perpendicular to the applied field. The results of these measurements are shown in Fig. 2. There is a noticeable peak in J_c for $H\sim H_{c2}$. This so-called "peak effect" has been observed in other superconductors.[35]

We note that the geometry $\vec{J}\perp\vec{H}$ is also the geometry appropriate for measurements of the dc flux-flow resistivity. However, because thermal instabilities occurred when using currents well above J_c, we were unable to determine the flux-flow resistivity experimentally.

The normal resistivity of Nb–26-at.% Hf was measured for $T=4.14$ K and $H>H_{c2}$, and was $\rho_n=34\pm2$ $\mu\Omega$ cm. This resistivity may be used to estimate certain quantities of interest, such as the electronic mean free path. To do this, however, calculations must be performed within the context of the free-electron model, since there are no band calculations for Nb–26-at.% Hf. In order to estimate the electronic density n, we make the usual approximation[7] and assume that each atom contributes a number of electrons equal to the number of valence electrons. For Nb this number is 5 and for Hf it is 4. With these approximations (and taking the electron mass equal

to the mass of the free electron) one obtains $n = 2.5 \times 10^{23}/\text{cm}^3$ and, for the Fermi velocity, $v_F = 2.3 \times 10^8$ cm/sec. For the sake of comparison, we did a similar calculation for Nb, obtaining $n = 2.7 \times 10^{23}/\text{cm}^3$ and $v_F = 2.3 \times 10^8$ cm/sec. We note, however, that Matthias,[36] starting from his band calculations for Nb, calculated an average Fermi velocity of $v_F = 5.1 \times 10^7$ cm/sec. Matthias pointed out, furthermore, that his value for v_F was in good agreement with experimental determination of this quantity.[36] If we suppose, therefore, that the band structure of Nb–26-at.% Hf is similar to that of Nb, our free-electron calculation for Nb suggests that we are actually overestimating the Fermi velocity for Nb–26-at.% Hf.

With these limitations in mind, we may use the previous values of n and v_F, and the measured value of ρ_n, to estimate the electronic relaxation time τ and mean free path l. We thus obtain $\tau \simeq 4 \times 10^{-15}$ sec, $l \simeq 9 \times 10^{-7}$ cm, and a BCS coherence length $\xi_0 = 3 \times 10^{-5}$ cm.

IV. RESULTS AND DISCUSSION

A. Comparison with microscopic theories

Previously[11] we encountered certain difficulties in comparing Nb–26-at.% Hf to the works of HM and CH. We encounter the same difficulties in comparing the attenuation of longitudinal waves (with $\vec{q} \perp \vec{H}$) with these theories. The problem is related to the proper identification of α_n, i.e., should we include the magnetic field dependence of the normal attenuation in α_n or should we take $\alpha_n = \alpha_n(H = 0)$. For longitudinal waves with $f = 20$ MHz, an estimate based upon the free-electron model[1] gives $\alpha_n(H = 0) \simeq 9 \times 10^{-4}$ dB/cm. However, as we mention previously, our method of estimating n and v_F almost certainly overestimates these quantities. It would, therefore, not be surprising if $\alpha_n(H = 0)$ were actually an order of magnitude smaller than our free-electron estimate. In any case, this value of α_n is much smaller than the observed H-induced changes in the attenuation for $H \gtrsim H_{c2}$, and is also smaller than the attenuation change between H_{c1} and H_{c2}. Thus the choice $\alpha_n = \alpha_n(H = 0)$ leads to the conclusion that $\alpha_s \gg \alpha_n$ for $H \simeq H_{c2}$, in gross disagreement with the theories of HM and CH.

We believe that it is more reasonable to take into account the H dependence of the normal attenuation in the definition of α_n. We therefore assume that α_n is the attenuation which would have existed at temperature T and field H, had the material been normal. To obtain this α_n, we note that the attenuation above H_{c2} is in good agreement with the AR theory.[14] According to this theory, α_n is proportional to H^2, for fields where $\alpha_n(H) \gg \alpha_n(H = 0)$, which is the case in our experiments for fields comparable to H_{c2}. We therefore calculate α_n at fields $0.5\, H_{c2} < H < H_{c2}$ by extrapolating the attenuation measured at $H > H_{c2}$ to lower fields. In Fig. 3 we show this extrapolation for shear waves. The extrapolation is carried out making a least-squares fit to the equation $\alpha = mH^2$, where m is a constant. The measured attenuation in the mixed state is identified with α_s. We thus compute $\Delta\alpha/\alpha_n \equiv (\alpha_n - \alpha_s)/\alpha_n$ and compare to the theories of HM and CH.

In the upper part of Fig. 4 we show values of $\Delta\alpha/\alpha_n$ determined in this fashion for longitudinal waves of various frequencies. We note some structure in the data near H_{c2}. The attenuation minimum (maximum in $\Delta\alpha/\alpha_n$) is related to the peak effect in the critical current[9] and is discussed in Sec. IV B. The physical origin of the small attenuation peaks which sometimes appear at slightly higher fields has been discussed in Sec. V A of Ref. 37. Note that for the experimental curves of lower frequencies, $\Delta\alpha/\alpha_n$ is always positive as predicted by HM and CH. However, for the highest frequency ($f = 45.3$ MHz), $\Delta\alpha/\alpha_n$ is negative for any value $H < H_{c2}$, in contradiction with these microscopic theories. Note also in Fig. 4 that the quantity $\Delta\alpha/\alpha_n$ is strongly dependent upon the ultrasonic frequency, and that this too is inconsistent with theory. We thus conclude that our experimental data cannot be interpreted in terms of the theories of HM and CH which neglect magnetohydrodynamic effects. We reached these same conclusions for shear waves[11] with $\vec{q} \| \vec{H}$, based on the lower half of Fig. 4 which shows the quantity $\Delta\alpha/\alpha_n$ for shear waves.

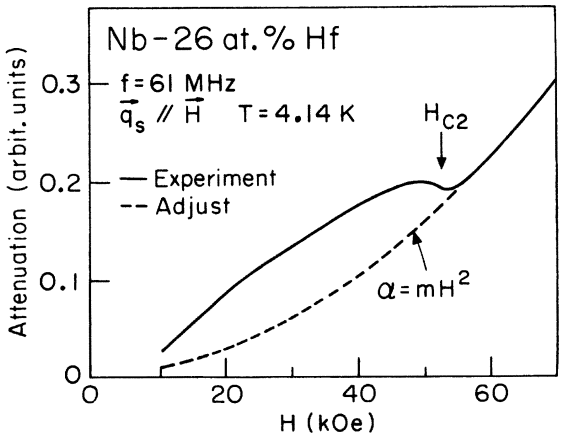

FIG. 3. Attenuation of 61-MHz shear waves vs H (solid curve). The normal attenuation α_n for $H < H_{c2}$ (dashed curve) was obtained by extrapolating the attenuation measured above H_{c2} using the relation $\alpha = mH^2$. It was assumed that the zero-field attenuation $\alpha_n(H = 0)$ was negligible.

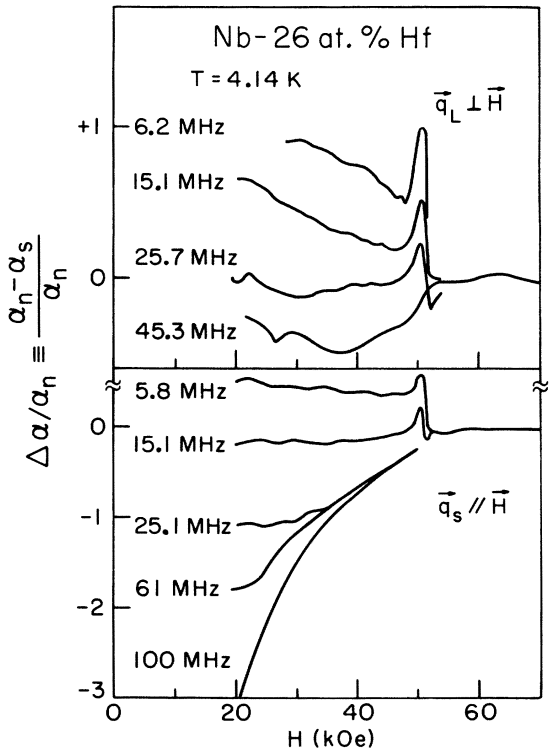

FIG. 4. Magnetic field dependence of the quantity $\Delta\alpha/\alpha_n = (\alpha_n - \alpha_s)/\alpha_n$ for several frequencies. The upper half of the figure is for longitudinal waves with $\vec{q}_L \perp \vec{H}$ and the lower half, for shear waves with $\vec{q}_S \parallel \vec{H}$.

At this point it is perhaps worthwhile to ask for the rational behind comparing our data to these theories. This question arises because the microscopic theories of HM and CH were constructed for clean materials where $l \gg \xi_0$, and not for "dirty" materials like Nb–26-at.% Hf. In answering this question we note that Tittman[7] has shown that the theories of HM and CH give a good qualitative understanding of the attenuation in materials of intermediate purity (V – 5.6-at.% Ta, where $l \sim \xi_0$) and of low purity (Mo–25-at.% Re, where $l < \xi_0$). It therefore seemed at least plausible that attenuation measurements in Nb–26-at.% Hf, a superconductor of low purity, might be explained in terms of these theories. The discrepancies which were observed between theory and experiment, however, are of a serious nature and cannot be explained simply by turning to a theory such as that of McClean and Houghton[38] which was constructed for very impure superconductors. We note that the "clean" theories of HM and CH and the "dirty" theory of McClean and Houghton differ with respect to the dependence of the attenuation on magnetic field, temperature and mean free path. These theories agree, however, on the point that the normal attenuation is always larger than the mixed-state attenuation. Thus the fact that $\Delta\alpha/\alpha_n$ is often negative for any $H < H_{c2}$ contradicts all these theories. To explain this aspect of our experimental curves it is necessary to consider magnetohydrodynamic effects, as SN did in their phenomenological model. It appears that the theories of HM, CH, and McClean and Houghton fail because they neglect magnetohydrodynamic effects.

B. Comparison with the model of SN

1. Magnetic field dependence

We now compare our experimental data with the model of SN. It will be convenient to consider the quantity α_s/α_n, where α_n is the H-induced change in the normal attenuation determined as in Fig. 3. In Fig. 5 we show α_s/α_n for 5.8 MHz shear waves propagating along the magnetic field. The theoretical curve denoted by ω_0 was calculated from Eq. (10), using the experimentally determined values of ω_0 calculated from J_c using Eq. (7). We see that the theoretical curve shows a minimum in the attenuation for fields slightly below H_{c2}. This minimum is related to the peak in the critical current for fields just below H_{c2} (see Fig. 2). On the

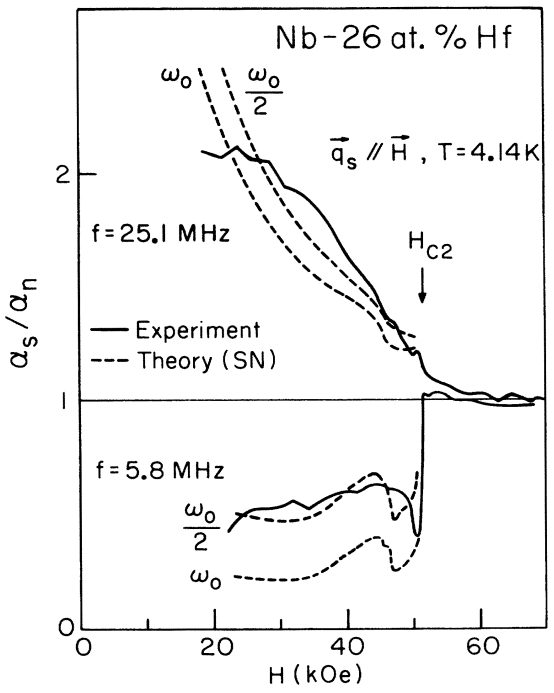

FIG. 5. Comparison of measured α_s/α_n vs H, for 5.8- and 25.1-MHz shear waves, with theoretical curves obtained from Eq. (10). Theoretical curves denoted by ω_0 were obtained by using the experimental values $f_0(H) = \omega_0(H)/2\pi$ of Fig. 2 in Eq. (10). The curves denoted by $\omega_0/2$ were obtained by dividing $f_0(H)$ by 2.

other hand, the curve denoted ω_0 differs considerably in magnitude from the experimental value for α_s/α_n for magnetic fields in the interval 25–50 kOe. In Fig. 5 we have also plotted a theoretical curve denoted by $\omega_0/2$ which was calculated using the experimentally-determined values $\omega_0(H)$, reduced by a factor of 2. This theoretical curve $\omega_0/2$ is in reasonably good agreement with the experimental values for α_s/α_n.

In Fig. 5 we also show α_s/α_n for shear waves with $f = 25.1$ MHz. In this case as well, we obtained somewhat better agreement between our experimental results and Eq. (10) by reducing the value ω_0 used to calculate α_s/α_n by a factor of 2. It is interesting to note also that the theoretical curve denoted ω_0 still shows a slight minimum associated with the peak in J_c. For the curve $\omega_0/2$, the effect of the peak in J_c is much reduced. For shear waves with frequencies greater than 25.1 MHz, the theoretical and experimental curves are very similar to those of Fig. 5. We will consider high-frequency results further in a later section.

In Fig. 6 we show α_s/α_n for longitudinal waves with $f = 15.6$ MHz. Here also reasonable agreement between the experimental data and Eq. (10) is obtained when we calculate α_s/α_n using the experimental values $\omega_0(H)$, reduced by a factor of 2.

In conclusion, there is a good qualitative agreement between our experimental data and Eq. (10). The observed minimum in the attenuation for magnetic fields just below H_{c2}, and which was attributed to the peak effect by Shapira and Neuringer, is predicted by Eq. (10) using experimentally determined values of ω_0. The magnitude of α_s/α_n, determined experimentally, agrees reasonably well with that calculated using Eq. (10), if we use values for ω_0 which are somewhat smaller than those determined experimentally. Generally speaking, a calculation of α_s/α_n made using $\omega_0/2$ agrees with the data for both shear and longitudinal waves.

2. *Frequency dependence*

We now consider the frequency dependence of the mixed-state attenuation, comparing the experimental determinations of α_s/α_n with the predictions of Eq. (10). We note that for high frequencies, where both $r \to 0$ and $\beta \gg 1$, this equation results in

$$\alpha_s/\alpha_n = \beta/\beta_f = H^*_{c2}(0)/H \quad (H_{c2} > H \gg H_{c1}) , \tag{21}$$

where the second equality is the result of using Eq. (6) for ρ_f. Equation (21) says that, for high frequencies, α_s/α_n is determined only by the ratio between H and $H^*_{c2}(0)$ and that it does not depend upon ω_0. For low frequencies, however, α_s/α_n should depend upon ω_0 and also upon β.

In Fig. 7 we compare α_s/α_n, determined experimentally for a field $H = 45$ kOe, with the same quantity calculated using Eq. (10). The curve designated as ω_0 was calculated using the experimental value of ω_0 and the curve $\omega_0/2$ was calculated with ω_0 reduced by a factor of 2. For high frequencies the two curves are identical, as expected from Eq. (21). In calculating these curves we used the value $H^*_{c2}(0) = 68.6$ kOe, determined from the slope dH_{c2}/dT near T_c. This value results in an excellent agreement between experi-

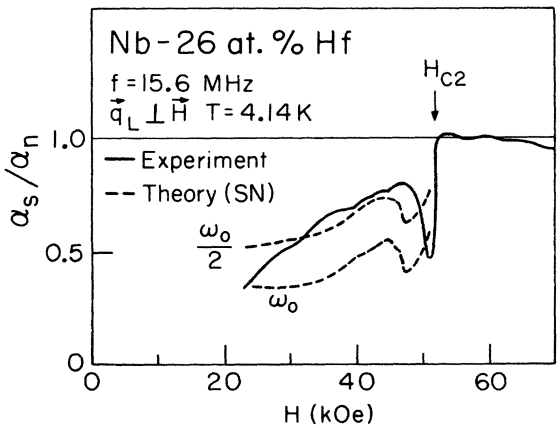

FIG. 6. Comparison of the measured H dependence of α_s/α_n for 15.6-MHz longitudinal waves with theoretical curves obtained from Eq. (10). The theoretical curve denoted by ω_0 was obtained by using the experimental values $f_0(H) = \omega_0(H)/2\pi$ of Fig. 2. The curve denoted $\omega_0/2$ was obtained by dividing $f_0(H)$ by 2.

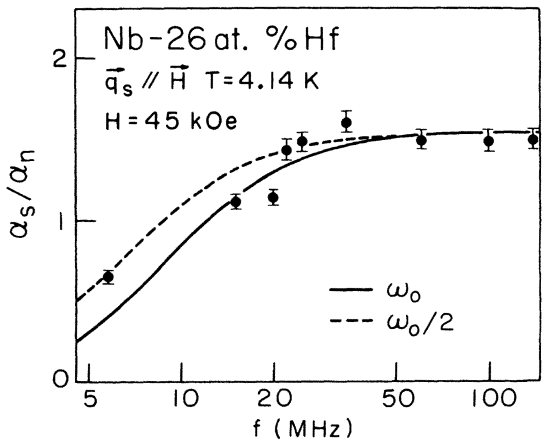

FIG. 7. Comparison of the frequency dependence of α_s/α_n for shear waves (full circles are experimental points) with the predictions of Eq. (10). The solid curve (denoted by ω_0) was obtained using the value f_0 (H = 45 kOe) from Fig. 2. The dashed curve (denoted by $\omega_0/2$) was obtained by dividing this f_0 (H = 45 kOe) by 2.

ment and the model of SN for high frequencies.

We should note, however, that the second equality of Eq. (21) results from using Eq. (6) for the flux-flow resistivity and that the latter equation was obtained supposing the upper critical field to be limited by paramagnetic effects, i.e., $H_{c2}(0) < H^*_{c2}(0)$. In the absence of paramagnetic effects, Eq. (6) should be written $\rho_f = \rho_n H/H_{c2}(0)$ and we have $\beta/\beta_f = H_{c2}(0)/H$ (for $H \gg H_{c1}$). In the case of Nb–26-at.% Hf, we have a situation where $H^*_{c2}(0)$, calculated from the slope dH_{c2}/dT near T_c, is smaller then $H_{c2}(0)$ (= 74.5 kOe). This result seems to suggest that the flow resistivity should be written using $H_{c2}(0)$. On the other hand we obtain better agreement between theory and experiment using $H^*_{c2}(0)$ in the calculation of α_s/α_n. The use of $H_{c2}(0) = 74.5$ kOe would increase the calculated α_s/α_n by ~10% for high frequencies and lead to a slight discrepancy between theory and experiment. We add, finally, that we obtain similar good agreement between the calculated and measured values for α_s/α_n not only at $H = 45$ kOe, but for all values of H above 25 kOe (below 25 kOe the uncertainity in the measured value of α_s is too large for a meaningful comparison).

For lower frequencies we note that α_s/α_n is somewhat more sensitive to the value of ω_0 used to calculate this quantity. However, the scatter in the experimental points of Fig. 7 makes it difficult to decide whether ω_0 or $\omega_0/2$ is more suitable in the calculation of α_s/α_n.

In Fig. 8 we show α_s/α_n obtained using longitudinal waves. The agreement between the experimental points and the theoretical curve calculated with $\omega_0/2$ is somewhat better than that calculated with ω_0.

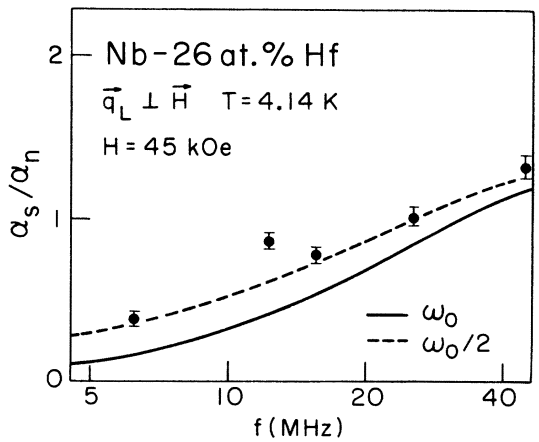

FIG. 8. Comparison of the frequency dependence of α_s/α_n for longitudinal waves (full circles are experimental points) with the predictions of Eq. (10). The solid curve (denoted by ω_0) was obtained by using the value f_0 (H =45 kOe) from Fig. 2. The dashed curve (denoted by $\omega_0/2$) was obtained by dividing f_0 (H =45 kOe) by 2.

Generally speaking we have observed an excellent qualitative agreement between our data and the model of SN. Although the theoretical curves for α_s/α_n are rather insensitive to the exact values of ω_0 (especially compared with the uncertainties in the experimental determination of α_s/α_n), the best quantitative fit to our data is obtained using $\omega_0/2$, where $\omega_0(H)$ is the set of values determined from J_c using Eq. (7). In any case, our data are not inconsistent with a single choice of $\omega_0(H)$ for both longitudinal and shear waves.

A careful examination of Eq. (10) shows that, for a fixed frequency, the quantity α_s/α_n depends only weakly upon $r = \omega_0/\omega$ when β is very large. Since $\beta \sim 1/V^2$, (where V is the zero-field sound velocity) the value of β (in Nb–26-at.% Hf) for shear waves is about 5 times larger than that for longitudinal waves *of the same frequency*. It is natural to expect, therefore, that α_s/α_n, for shear waves, depends more weakly upon r (and, therefore, upon ω_0) than for longitudinal waves of the same frequency. This explains, for example, why the minimum in the attenuation associated with the peak effect is still visible for longitudinal waves with $f = 45.3$ MHz and, on the other hand, is not observed using shear waves with $f = 34.6$ MHz (see Ref. 26). Previously, SN had suggested the existence of two characteristic frequencies ω_0, one for shear waves and the other for longitudinal waves. We see, however, that this is unnecessary in the present case and that a single characteristic frequency is probably sufficient to explain all data for both shear and longitudinal waves.

C. Comparison with the modified model

In this section we wish to compare our data with a modification of the model of SN which gives a better description of α_s/α_n for high frequencies and for magnetic fields close to H_{c2}. The necessity of this modification is clear once we note that the model of SN predicts a discontinuity in the attenuation for $H \lesssim H_{c2}$, which is, in turn, the result of an apparent discontinuity in the resistivity of the material for fields in the vicinity of H_{c2}. As we mentioned previously, however, Eq. (6) is not valid for fields in the vicinity of H_{c2}.[19,21,22] Therefore, the use of Eq. (6) for the flux-flow resistivity in the model of SN may lead to inaccurate results near H_{c2}.

A more rigorous expression for the flux-flow resistivity was obtained by Thompson.[15] Thompson's result, which should be valid for fields in the vicinity of H_{c2} and for frequencies such that the pinning forces may be neglected, was used in Sec.

II B as an effective resistivity in the AR theory. There, we obtained an expression for α_s/α_n given by Eq. (18). Since the frequencies $f_0(H)$ characteristic of the pinning forces are in the range 10–15 MHz for our Nb–26-at.% Hf sample at $T=4.14$ K, it seems reasonable that, for higher frequencies, such as 60–140 MHz, the pinning forces will not be important and Eq. (18) should give a good description of the mixed-state attenuation.

In order to compare our experimental determinations of α_s/α_n with Eq. (18), it is necessary to determine the parameter γ given by Eq. (16). To calculate γ we took $N=\frac{1}{3}$ for our approximately cubical sample and used our previous estimate $\kappa_2 \simeq 7.4$. Since $L_D(t)$ varies smoothly between the values 1 and 2, we made the approximation $L_D(t) \simeq 1.5$ for $T=4.14$ K. Then using the values of ρ_n, l, and v_F of Sec. III, we obtained $\gamma \simeq 0.5$. Since $D=\frac{1}{3}v_F l \sim n^{-1/3} \sim v_F^{-1/3}$, it is probable that γ should be somewhat smaller than this estimate.

Finally, in Fig. 9, we compare α_s/α_n, determined experimentally for shear waves with $f=100$ MHz, with the same quantity calculated using Eq. (10) (curve designated SN) and also using Eq. (18) (curve designated revised theory). As we note in Fig. 9, the model of SN [Eq. (10)] fails near H_{c2} since this equation predicts a discontinuity in α_s/α_n for $H=H_{c2}$ which is not observed experimentally. This prediction cannot be modified by varying ω_0 since for high frequencies, α_s/α_n, calculated from Eq. (10) is independent of ω_0. As we mentioned previously, this discontinuity is connected with the apparent discontinuity in ρ_f suggested by Eq. (6). We note also that Eqs. (15) and (19) indicate that α_s/α_n may be determined directly from the flux-flow resistivity. However, as we mentioned previously in Sec. III, we were unable to measure the flux-flow resistivity near H_{c2} because of heating at currents above the critical current.

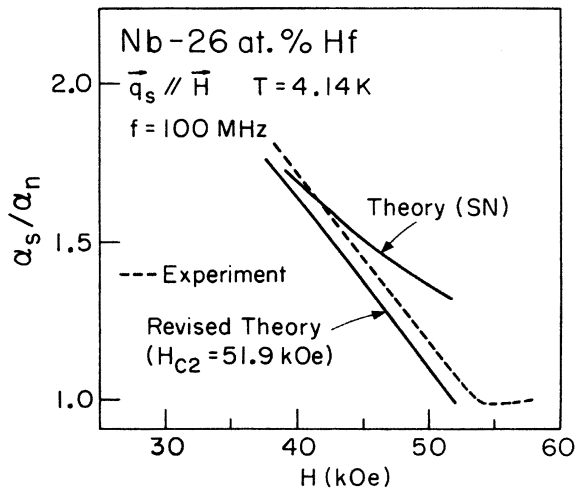

FIG. 9. Comparison of the measured H dependence of α_s/α_n for 100-MHz shear waves with theory of SN [Eq. (10)] and revised theory [Eq. (18)].

Also in Fig. 9, we have calculated α_s/α_n using Eq. (18) with $\gamma=3.2$ and $H_{c2}=51.9$ kOe. This value of γ reproduces the slope of the experimental curve but is larger than our previous *a priori* estimate of this quantity. Concerning this discrepancy in the value of γ, it should be noted that there are difficulties involved in estimating the mean free path and the Fermi velocity, which enter into our estimate of γ. Thus, it is not surprising that agreement of this estimate with that obtained experimentally is only an order of magnitude agreement.

We notice also that plotting the theoretical curve with $H_{c2}(T=4.14\text{ K})=51.9$ kOe results in its being offset slightly from the experimental curve. On the other hand, using $H_{c2}(4.14\text{ K})=53.4$ kOe, the theoretical and experimental curve coincide. The value 51.9 kOe was determined experimentally from our resistivity measurements using a somewhat arbitrary criterion for H_{c2}. Since the width of the resistive transition at 4.14 K is about 1.5 kOe, a value of 53.4 kOe for H_{c2} is also consistent with our experimental determination of H_{c2}.

We note also that our experimental curves of α_s/α_n, obtained with shear waves with $f=61$ MHz and $f=140$ MHz, are also in good agreement with Eq. (19) when we use the same value for γ, namely, $\gamma=3.2$, and $H_{c2}=51.9$ kOe. Thus the slope of α_s/α_n seems to be independent of the ultrasonic frequency, as Eqs. (19) and (16) suggest. To see to what extent our modification of the SN theory is useful we have compared Eq. (19) to a curve of α_s/α_n obtained with shear waves with $f=25.1$ MHz. Although pinning forces are clearly important in this frequency range, a reasonable agreement was obtained between experiment and theory using $\gamma=2.6$. Thus it appears that the revised theory can give a reasonable account of the data into the frequency range where ω is comparable to ω_0. The modified theory was not compared with longitudinal-wave attenuation because the effects of pinning forces were always present for the frequencies studied and β was always small.

V. CONCLUSIONS

We have compared our attenuation data with the microscopic theories of HM and CH for the mixed-state attenuation. These theories predict that $\Delta\alpha/\alpha_n$ is always positive and is independent of frequency for $ql<1$. Our data contradict these theories in these two respects and would also be in contradiction to other theories, such as that of

McClean and Houghton which was constructed for very impure superconductors but which neglected magnetohydrodynamic effects. The necessity of considering these effects is one of the important results of this work.

On the other hand, our data are in good agreement with the phenomenological model of SN where magnetohydrodynamic effects are taken into account. We have studied the predictions of this model with respect to the dependence of the attenuation of magnetic field and frequency. In qualitative terms, the agreement between the model and our data is excellent, with the model predicting all of the characteristics of the experimental curves. Our measurements are consistent with an interpretation in terms of a single characteristic frequency ω_0 for both longitudinal and shear waves. In fact, a careful examination of Eq. (10) shows that the dependence of the attenuation on ω_0 is different for shear and longitudinal waves of the same frequency. It is not, therefore, necessary to have recourse to two characteristic frequencies ω_0, one for shear waves and the other for longitudinal waves, as previously suggested by SN.

Our modification of the model of SN consists in using Thompson's expression for the flux-flow resistivity[15,23] as an effective resistivity in the AR theory. Our modification which should be valid for $H \sim H_{c2}$ and for high frequencies such that the pinning forces may be neglected, eliminates the discontinuity in α_s/α_n at H_{c2} which was predicted by the model of SN. Also, the observed linear behavior of α_s/α_n with $(H_{c2}-H)$ near H_{c2} is a natural consequence of our modification. Our *a priori* estimate of the slope γ is lower than the value necessary to fit our experimental data. However, this difficulty seems understandable, given the difficulties in estimating v_F, l, and κ_2 for Nb–26-at.% Hf. We note that γ should depend rather strongly upon temperature. This is especially true if we are correct in assuming that Thompson's expression for the flux-flow resistivity may be used in the AR theory. Work is currently under way to test this aspect of the model.

Note added in proof. We have recently measured the attenuation of 50-MHz shear waves (with $\vec{q} \| \vec{H}$) in V–42-at.% Ti at several temperatures $1.5 < T < 4.2$ K. The object of these measurements was to determine the temperature dependence of the parameter γ which describes the behavior of the attenuation near H_{c2} [see Eq. (19)]. The inequalities $\beta \gg 1$ and $\omega \gg \omega_0$, assumed in deriving Eq. (19) were satisfied in these experiments.[9] We found that γ increases with decreasing T in disagreement with Eq. (16). It thus appears that further theoretical work is necessary for a detailed understanding of the attenuation near H_{c2}.

ACKNOWLEDGMENTS

The authors would like to thank Dr. L. J. Neuringer for the sample used in these experiments.

---

*Supported by Fundação de Amparo à Pesquisa do Estado de São Paulo.

†Work supported in part by a joint grant from NSF (USA) and Conselho Nacional de Desenvolvimento Científico e Tecnológico (Brasil).

‡Present address: Francis Bitter National Magnet Laboratory, MIT, Cambridge, Mass.

§Supported by the National Science Foundation.

[1]R. W. Morse, in *Progress in Cryogenics*, edited by K. Mendelssohn (Heywood, London, 1959), Vol.I, p. 219.

[2]M. Gottlieb, M. Garbuny, and C. K. Jones, in *Physical Acoustics*, edited by Warren P. Mason and R. N. Thurston (Academic, New York, 1970), Vol. VII, p. 1.

[3]A. Houghton and K. Maki, Phys. Rev. B 4, 843 (1971).

[4]H. A. Cerdeira and A. Houghton, Phys. Rev. B 3, 2997 (1971).

[5]F. Carsey and M. Levy, Phys. Rev. Lett. 27, 853 (1971).

[6]J. A. Waynert, H. Salvo, Jr., and M. Levy, Phys. Rev. B 10, 1859 (1974).

[7]B. R. Tittman, in Proceedings of the 1974 I.E.E.E. Ultrasonics Symposium, I.E.E.E. Cat. No. 74 CHO 896-1 SU, p. 449.

[8]M. Ashkin, D. W. Deis, M. Gottlieb, and C. K. Jones, Physica 55, 631 (1971).

[9]Y. Shapira and L. J. Neuringer, Phys. Rev. 154, 375 (1967).

[10]Y. Shapira, in *Physical Acoustics*, edited by W. P. Mason (Academic, New York, 1968), Vol. V, p. 1.

[11]F. P. Missell, N. F. Oliveira, Jr., and Y. Shapira, Solid State Commun. 18, 1553 (1976).

[12]J. I. Gittleman and B. Rosenblum, Phys. Rev. Lett. 16, 734 (1966).

[13]G. E. Possin and K. W. Shepard, Phys. Rev. 171, 458 (1968).

[14]R. A. Alpher and R. J. Rubin, J. Acous. Soc. Amer. 26, 452 (1954).

[15]R. S. Thompson, Phys. Rev. B 1, 327 (1970).

[16]C. Caroli and K. Maki, Phys. Rev. 159, 306 (1967).

[17]C. Caroli and K. Maki, Phys. Rev. 164, 591 (1967).

[18]H. Takayama and H. Ebisawa, Prog. Theor. Phys. 44, 1450 (1970).

[19]Y. B. Kim, C. F. Hempstead, and A. R. Strnad, Phys. Rev. 139, A1163 (1965).

[20]L. A. Vienneau and B. W. Maxfield, Phys. Rev. B 11, 4339 (1975).

[21]C. J. Axt and W. C. H. Joiner, Phys. Rev. 171, 461 (1968).

[22]Y. Muto, K. Mori, and K. Noto, Physica 55, 362 (1970).

[23]R. J. Pedersen, Y. B. Kim, and R. S. Thompson, Phys. Rev. B 7, 982 (1973).
[24]K. Maki and T. Tsuzuki, Phys. Rev. 139, A868 (1965).
[25]E. P. Papadakis, J. Appl. Phys. 35, 1474 (1964).
[26]F. P. Missell, N. F. Oliveira, Jr., and Y. Shapira, in Ref. 7, p. 441.
[27]O. L. Anderson, J. Phys. Chem. Solids 24, 909 (1963).
[28]J. K. Hulm and R. D. Blaugher, Phys. Rev. 123, 1569 (1961).
[29]K. Maki, Physics 1, 127 (1964); Phys. Rev. 148, 362 (1966).
[30]N. R. Werthamer, E. Helfand, and P. C. Hohenberg, Phys. Rev. 147, 295 (1966).
[31]R. E. Somekh, J. Phys. F 4, 2231 (1974).
[32]R. G. Hampshire and M. T. Taylor, J. Phys. F 2, 89 (1972).
[33]R. B. Laibowitz, V. Sadagopan, and P. E. Seiden, Phys. Lett. 31A, 133 (1970).
[34]W. L. McMillan, Phys. Rev. 167, 331 (1968).
[35]See E. J. Kramer, J. Appl. Phys. 44, 1360 (1973), and references cited therein.
[36]L. F. Matthias, Phys. Rev. B 1, 373 (1970).
[37]L. J. Neuringer and Y. Shapira, Phys. Rev. 148, 231 (1966).
[38]F. B. McClean and A. Houghton, Phys. Rev. 157, 350 (1967).